Filtering out high frequencies in time series using F-transform[☆]

Vilém Novák[c], Irina Perfilieva[c], Michal Holčapek[c], Vladik Kreinovich[d]

[a] *University of Ostrava*
Institute for Research and Applications of Fuzzy Modelling,
NSC IT4Innovations
30. dubna 22, 701 03 Ostrava 1, Czech Republic

[b] *Department of Computer Science*
University of Texas at El Paso
500 W. University, El Paso, TX 79968, USA

Abstract

In this paper, we focus on application of fuzzy transform (F-transform) to analysis of time series under the assumption that the latter can be additively decomposed into trend-cycle, seasonal component and noise. We prove that when setting properly width of the basic functions, the inverse F-transform of the time series closely approximates its trend-cycle. This means that the F-transform almost completely removes the seasonal component and noise. The obtained theoretical results are demonstrated on two artificial time series whose trend cycle is precisely known and on three real time series. At the same time, comparison with three classical methods, namely STL-method, SSA-method and low pass Butterworth filter is also provided.

Keywords: Fuzzy transform, F-transform, time series, decomposition model.

[☆]This work relates to Department of the Navy Grant N62909-12-1-7039 issued by Office of Naval Research Global. The United States Government has a royalty-free license throughout the world in all copyrightable material contained herein. Additional support was given also by the European Regional Development Fund in the IT4Innovations Centre of Excellence project (CZ.1.05/1.1.00/02.0070).

Email addresses: Vilem.Novak@osu.cz (Vilém Novák), Irina.Perfilieva@osu.cz (Irina Perfilieva), Michal.Holcapek@osu.cz (Michal Holčapek), vladik@utep.edu (Vladik Kreinovich)

Filtering out high frequencies in time series using F-transform[☆]

Vilém Novák[c], Irina Perfilieva[c], Michal Holčapek[c], Vladik Kreinovich[d]

[c] *University of Ostrava*
Institute for Research and Applications of Fuzzy Modelling,
NSC IT4Innovations
30. dubna 22, 701 03 Ostrava 1, Czech Republic

[d] *Department of Computer Science*
University of Texas at El Paso
500 W. University, El Paso, TX 79968, USA

1. Introduction

This paper is devoted to analysis of time series using fuzzy transform (in short, F-transform). The theory and methods of the latter were introduced in [19] and further elaborated in [20, 21]. Application of the F-transform to analysis and forecasting of time series was first published in [18] and then further elaborated in [16, 17].

From the very beginning it was clear that the F-transform is a promising technique that can be effectively applied to extraction of the trend(-cycle). Clear mathematical proof, however, was not provided. In this paper, we fill this gap and give the missing mathematical justification. In accordance with the standard approach, we assume that a time series can be additively decomposed into a trend-cycle TC, a seasonal component S and a random noise R (cf., for example, [2]).

The motivation for our analysis comes from the following general characterization of a trend-cycle of a time series taken from the OECD Glossary of Statistical Terms:

> *The trend-cycle of a time series is the component that represents variations of low frequency in a time series, the high frequency fluctuations having been filtered out. This component can be viewed as*

[☆] This work relates to Department of the Navy Grant N62909-12-1-7039 issued by Office of Naval Research Global. The United States Government has a royalty-free license throughout the world in all copyrightable material contained herein. Additional support was given also by the European Regional Development Fund in the IT4Innovations Centre of Excellence project (CZ.1.05/1.1.00/02.0070).

Email addresses: Vilem.Novak@osu.cz (Vilém Novák), Irina.Perfilieva@osu.cz (Irina Perfilieva), Michal.Holcapek@osu.cz (Michal Holčapek), vladik@utep.edu (Vladik Kreinovich)

those variations with a period longer than a chosen threshold (usually 1 year is considered as the minimum length of the business cycle).

This characterization provides the basic idea without formal explication of the used terms. A more detailed inspection of it reveals the assumption that the time series can be decomposed as outlined above. The trend-cycle can be represented by a sufficiently smooth function without clear periodicity or it can be periodic but with periodicity significantly longer than any of the periodicities forming the seasonal component S. Therefore, we will assume that the seasonal component S is a mixture of periodic functions, while the trend-cycle TC can be arbitrary. In this paper, we will show that using the F-transform, we can filter out the seasonal component S and significantly reduce the noise R. What remains is the trend-cycle.

Standard statistical methods used in the analysis of time series assume that the trend-cycle is formed by some, usually simple, function (quite often a linear one) that is usually extracted using regression analysis (cf. [13]). We argue that this approach is dubious since one can hardly suppose that the trend-cycle TC takes a simple course on the whole domain. As will be seen later, the F-transform makes it possible to consider the trend-cycle TC to be a function of arbitrary shape and thus, to extract TC in its true form, whatever it is. At the same time, it provides also analytic expression for TC. Let us remark that our technique, in some sense, can be ranked among non-parametric techniques that are usually used in time series analysis if an explicitly given shape of components cannot be assumed (see, [6, 7, 14]). A survey of techniques including filter theory used in time series analysis can be found in [26].

Other classical methods providing decomposition of time series are STL and SSA-methods (see [4, 8, 11]). It can be demonstrated (see below) that estimation of TC using both of them is comparable with that obtained using the F-transform. The arguments in favor of the F-transform, however, are its transparentness, simplicity and significantly less computational complexity in comparison with the STL and SSA methods. Namely, the computational complexity of the F-transform is linear (see [22]), while the SSA-methods requires computation of eigenvalues and eigenvectors of lag-covariance matrix that is very expensive especially when long time series are analyzed. Thus, the computational complexity of the regression models is at least square and computation of eigenvalues has cubic complexity.

The problem solved in this paper is similar to signal filtering, where we also face the task to remove high frequencies present as noise in a signal. Our approach, however, differs from the classical signal filtering theory, where it is assumed that the function is formed of (infinite) number of sinusoidal functions and filtering is based on removing functions with high frequencies (cf. [24]). Last but not least, the F-transform is computationally simple and so, very fast algorithms were developed. Note that results of this paper extend the results from [15, 23].

The structure of this paper is the following. In Section 2, we briefly overview the main notions of the F-transform theory with the focus to the properties

needed further. The main part of the paper is Section 3, where we prove that under specific conditions, the F-transform filters out seasonal component consisting of high frequencies and reduces the random noise so that only the trend-cycle TC remains. In Section 4, we demonstrate theoretical results obtained in this paper on two artificial times series whose structure is thus precisely known and on three real time series. At the same time, we compare F-transform with the above mentioned STL and SSA-methods, as well as low pass Butterworth filter.

2. Preliminaries

In this section, we will briefly review the main principles of the F-transform. Detailed explanation of the general theory can be found in [19, 20, 21].

Let U be an arbitrary (nonempty) set called a *universe*. By a *fuzzy set* in the universe U we will understand a function $A : U \longrightarrow [0, 1]$. By $\mathscr{F}(U)$ we denote the set of all fuzzy sets on U.

The F-transform is essentially a linear mapping that assigns a finite vector of specially computed components to a given function f (continuous or discrete). We will work with the integral form of the F-transform that maps the set $C([a, b])$ of real continuous functions to the set R^n. The inverse F-transform is again a linear mapping from R^n to $C([a, b])$ such that being applied to the direct F-transform of f, it gives a function that approximates the original function f. This seeming disadvantage can be turned out into great advantage since by proper setting of the parameters we can obtain a function with the desired properties.

There are F-transforms of zero and higher degree. In the first case, the target space is the vector space $\mathbb{R}^n$ and the transformation $C([a, b]) \longrightarrow \mathbb{R}^n$ is specified by a *fuzzy partition* of the interval $[a, b]$. The higher degree F-transform maps a function from $C([a, b])$ to a finite vector of polynomial components. In this paper, we will consider only the first-degree F-transform where the components are linear polynomials.

2.1. F^0-transform

Let us consider a function $f \in C([a, b])$. To apply the F-transform, we must first specify a *fuzzy partition* of $[a, b]$.

Definition 1
Let $n \in \mathbb{N}$, $n \geq 2$, be given and $c_0 < \ldots < c_n$ be fixed nodes within $[a, b]$, such that $c_0 = a, c_n = b$. We say that fuzzy sets $A_0, \ldots, A_n \in \mathscr{F}([a, b])$ form a fuzzy partition of $[a, b]$ *if they satisfy the following conditions for $k = 0, \ldots, n$:*

1. *$A_k(c_k) = 1$;*
2. *$A_k(x) = 0$ for $x \notin (c_{k-1}, c_{k+1})$, $k = 0, \ldots, n$ where we formally put $c_{-1} = a$ and $c_{n+1} = b$;*
3. *A_k is continuous;*

4. *A_k strictly increases on $[c_{k-1}, c_k]$ and strictly decreases on $[c_k, c_{k+1}]$;*

5. *for all $x \in [a, b]$,*

$$\sum_{k=0}^{n} A_k(x) = 1. \tag{1}$$

The fuzzy sets $A_0, \ldots, A_n$ are in the theory of F-transform called *basic functions*. The most common is *uniform fuzzy partition*.

Definition 2
Let $A_0, \ldots, A_n$ be a fuzzy partition of $[a, b]$. We say that it is uniform *if the following is satisfied:*

(i) The nodes $c_0 = a, \ldots, c_n = b$ are h-equidistant, i.e. $c_k = a + kh$, $k = 0, \ldots, n$ where $h = \frac{b-a}{n}$.

(ii) The basic functions are symmetric, i.e. $A_k(c_k - x) = A_k(c_k + x)$ for all $x \in [0, h]$ and $k = 1, \ldots, n-1$.

(iii) The following holds for all $k = 1, \ldots, n-1$ and $x \in [x_k, x_{k+1}]$:

$$A_k(x) = A_{k-1}(x - h),$$
$$A_{k+1}(x) = A_k(x - h).$$

Let us remark that shapes of the basic functions are not predetermined and can be chosen on the basis of additional requirements. In the following text, we will always *assume that the considered fuzzy partition is uniform*. By width of a fuzzy set A_k we understand the width of its support. In case of the uniform fuzzy partition, the width of each A_k is $2h$ (except for A_0 and A_n where it is h).

In this paper, we will work with triangular fuzzy sets defined by:

$$A_k(t) = \begin{cases} \frac{t - c_{k-1}}{h}, & t \in [c_{k-1}, c_k], \\ \frac{c_{k+1} - t}{h}, & t \in [c_k, c_{k+1}] \end{cases} \tag{2}$$

for all $k = 0, \ldots, n$ (for A_0 and A_n, we consider in (2) only the interval $[c_0, c_1]$ and $[c_{n-1}, c_n]$, respectively). Note also that $\int_{c_{k-1}}^{c_{k+1}} A_k(x)dx = h$ and $\int_{c_k}^{c_{k+1}} A_k(x)dx = \frac{h}{2}$.

It should be noted that the fuzzy transform can also be defined with respect to a more general fuzzy partition, in which some of the conditions of Definition 1 are relaxed, for example condition 5. The details can be found in [12].

Definition 3
Let a fuzzy partition of $[a, b]$ be given by basic functions $A_0, \ldots, A_n, n \geq 2$, and let $f : [a, b] \longrightarrow \mathbb{R}$ be from $C([a, b])$. The $(n+1)$-tuple of real numbers $\mathbf{F}[f] = (F_0[f], \ldots, F_n[f])$ given by

$$F_k[f] = \frac{\int_a^b f(x)A_k(x)dx}{\int_a^b A_k(x)dx}, \qquad k = 0, \ldots, n, \tag{3}$$

is called the direct fuzzy transform (F-transform) *of f with respect to the given fuzzy partition. The numbers $F_0[f], \dots, F_n[f]$ are called components of the F-transform of f.*

In case that the partition is h-uniform, computation of the components can be simplified as follows:

$$F_0[f] = \frac{2}{h}\int_{c_0}^{c_1} f(x)A_1(x)dx \quad \text{and} \quad F_n[f] = \frac{2}{h}\int_{c_n-1}^{c_n} f(x)A_n(x)dx, \tag{4}$$

$$F_k[f] = \frac{1}{h}\int_{c_{k-1}}^{c_{k+1}} f(x)A_k(x)dx, \qquad k = 1, \dots, n-1. \tag{5}$$

It should be noted that the components of the F^0-transform are weighted mean values of the original function, where the weights are determined by the basic functions; see, e.g., [19].

In practice, the function f is often given not analytically but in the form of a table that contains results of some measurements. In this case, Definition 3 must be modified in such a way that the definite integrals in (3) are replaced by finite summations. In this case, we speak about *discrete F-transform*.

The F-transform of f with respect to the fuzzy partition $A_0, \dots, A_n$ will be denoted by $\mathbf{F}[f] = (F_0[f], \dots, F_n[f])$. If the function f is clear from the context then the "$[f]$" in $F_i[f]$ can be omitted.

As can be seen from (4), the boundary components $F_0[f]$ and $F_n[f]$ are computed using only ss of the basic functions. Therefore, we will often consider the F-transform only as the vector of inner components $\overline{\mathbf{F}}[f] = [F_1[f], \dots, F_{n-1}[f]]$.

Important property of the F-transform is its linearity; namely, if $h = \alpha f + \beta g \in C[a, b]$ then

$$\mathbf{F}[h] = \alpha[f] + \gamma\mathbf{F}[g].$$

The original function f can be approximately reconstructed from $\mathbf{F}[f]$ using the following inversion formula.

Definition 4
Let $\mathbf{F}[f]$ be the direct F-transform of f with respect to the fuzzy partition $A_0, \dots, A_n \in \mathscr{F}([a, b])$. Then the function $\hat{f}$ given on $[a, b]$ by

$$\hat{f}(x) = \sum_{k=0}^{n} F_k[f] \cdot A_k(x), \tag{6}$$

is called the inverse F-transform[1] *of f.*

The inverse F-transform $\hat{f}$ is a continuous function on $[a, b]$. Moreover, the linearity property holds for it too, i.e., if $h = \alpha f + \beta g \in C[a, b]$ then

$$\hat{h} = \alpha\hat{f} + \gamma\,\hat{g}$$

[1]We will use the term "inverse F-transform" in two meanings: (a) as the procedure for obtaining the estimation of f and (b), as the resulting function (6) approximating f.

provided that the fuzzy partition is fixed. For various properties of the F-transform and detailed proofs — see [19].

In our analysis below we will also consider the case when $f : [a, b] \longrightarrow \mathbb{C}$ being a complex-valued function of a real variable. In this case, we will write the direct F-transform of f as

$$\mathbf{F}[f] = \mathbf{F}[Re(f)] + i\,\mathbf{F}[Im(f)].$$

Hence, the inverse F-transform of f becomes

$$\hat{f} = Re(\hat{f}) + i\,Im(\hat{f}),$$

or in more detail

$$\hat{f}(x) = \sum_{k=0}^{n} F_k[Re(f)] \cdot A_k(x) + i \sum_{k=0}^{n} F_k[Im(f)] \cdot A_k(x).$$

2.2. F^m-transform

The F-transform can be further generalized. Namely, we can introduce higher-degree F-transform (F^m-transform, $m \geq 0$). Its components are polynomials of degree m. Thus, the original F-transform described above coincides with the F^0-transform (zero-degree F-transform). Below, we will overview the main points of the F^m-transform. Detailed definitions, theorems and their proofs can be found in [21] where the F^m-transform was introduced.

Let us fix an interval $[a, b]$ of reals. The fuzzy partition will be taken over "full" fuzzy sets, i.e. we will consider only $A_1, \ldots, A_{n-1} \in \mathscr{F}([a, b])$, $n \geq 2$. Let k be a fixed integer from $\{1, \ldots, n-1\}$, and $L_2(A_k)$ be a Hilbert space of square-integrable functions $f : [x_{k-1}, x_{k+1}] \longrightarrow \mathbb{R}$ with the scalar product

$$\langle f, g \rangle_k = \frac{\int_{x_{k-1}}^{x_{k+1}} f(x)g(x)A_k(x)dx}{\int_{x_{k-1}}^{x_{k+1}} A_k(x)dx}.$$

By $L_2(A_1, \ldots, A_{n-1})$ we denote a set of functions $f : [a, b] \longrightarrow \mathbb{R}$ such that $f|_{[c_{k-1}, c_{k+1}]} \in L_2(A_k)$ for all $k = 1, \ldots, n-1$.

Definition 5
Let $f : [a, b] \longrightarrow \mathbb{R}$ be a function from $L_2(A_1, \ldots, A_{n-1})$ and $m \geq 0$ be a fixed integer. We say that the n-tuple of polynomials $\mathbf{F}^m[f] = (F_1^m[f], \ldots, F_{n-1}^m[f])$ is an F^m-transform *of f with respect to the fuzzy partition $A_0, \ldots, A_n$ if*

$$F_k^m[f] = \beta_k^0 P_k^0 + \beta_k^1 P_k^1 + \cdots + \beta_k^m P_k^m,$$

where

$$\beta_k^i = \frac{\int_a^b f(x)P_k^i(x)A_k(x)dx}{\int_a^b P_k^i(x)P_k^i(x)A_k(x)dx}, \quad i = 0, \ldots, m$$

and P_k^i are orthogonal polynomials of i-th order. The polynomial $F_k^m[f]$ is called k-th F^m-transform component *of f.*

Each component approximates f in a certain area. Thus, the quality of approximation increases with the increase of the degree of the polynomials. The following can be proved:

(a) Each F^m-transform component $F_k^m[f]$, $k = 0, \ldots, n$, minimizes the functional

$$\Phi_k(g) = \int_a^b (f(x) - g(x))^2 A_k(x) dx, \tag{7}$$

defined on elements $g \in L_2^m(A_k)$.

(b) If f is a polynomial of degree $l \leq m$ then each F^m-transform component $F_k^m[f]$, $k = 1, \ldots, n-1$ restricted to $[c_{k-1}, c_{k+1}]$ coincides with f on $[c_{k-1}, c_{k+1}]$.

(c) Each F^m-transform component $F_k^m[f]$, $k = 1, \ldots, n-1$, satisfies the following recurrent equation:

$$F_k^m[f] = F_k^{m-1}[f] + \beta_k^m P_k^m, \quad m = 1, 2, \ldots. \tag{8}$$

(d) The F^m-transform of f is linear, i.e.

$$\mathbf{F}^m[\alpha f + \gamma g] = \alpha \mathbf{F}^m[f] + \gamma \mathbf{F}^m[g],$$

holds for all $f, g \in L_2(A_1, \ldots, A_{n-1})$, and for all $\alpha, \beta \in \mathbb{R}$, where the equality is considered over the respective vectors of components.

The following theorem characterizes the F^1-transform of f with respect to a h-uniform fuzzy partition $A_0, \ldots, A_n$. Its proof can be found in [21].

Theorem 1
The vector of linear functions

$$\mathbf{F}^1[f] = (\beta_1^0 + \beta_1^1(x - c_0), \ldots, \beta_{n-1}^0 + \beta_{n-1}^1(x - c_{n-1})) \tag{9}$$

is the F^1-transform of f with respect to the h-uniform fuzzy partition $A_1, \ldots, A_{n-1}$, where

$$\beta_k^0 = \frac{\int_{c_{k-1}}^{c_{k+1}} f(x) A_k(x) dx}{h}, \tag{10}$$

$$\beta_k^1 = \frac{\int_{c_{k-1}}^{c_{k+1}} f(x)(x - c_k) A_k(x) dx}{\int_{c_{k-1}}^{c_{k+1}} (x - c_k)^2 A_k(x) dx}, \tag{11}$$

for every $k = 1, \ldots, n-1$.

Note that $\beta_k^0 = F_k^0[f]$ where $F_k^0[f]$ is the component (5) (we added the superscript 0 to emphasize that Definition 3, in fact, introduces zero degree F-transform).

Corollary 1
If the partition $A_0, \ldots, A_n$ is uniform and the basic functions A_k have triangular shape then (11) becomes

$$\beta_k^1 = \frac{12 \int_{c_{k-1}}^{c_{k+1}} f(x)(x - c_k)A_k(x)dx}{h^3} \tag{12}$$

Similarly to the original F-transform, the inverse F^m-transform of a function f is defined as a linear combination of basic functions with "coefficients" given by the F^m-transform components.

Definition 6
Let $f : [a, b] \longrightarrow \mathbb{R}$ be a given function, $m \geq 0$ and $\mathbf{F}^m[f] = (F_1^m[f], \ldots, F_{n-1}^m[f])$ be the F^m-transform of f with respect to the fuzzy partition $A_1, \ldots, A_{n-1}$. Then the function $\hat{f}^m : [a, b] \longrightarrow \mathbb{R}$ defined by

$$\hat{f}^m(x) = \sum_{k=1}^{n-1} F_k^m[f](x)A_k(x) \tag{13}$$

is called inverse F^m-transform *of f with respect to $\mathbf{F}^m[f]$ and $A_0, \ldots, A_n$.*

The following recurrent formula can be applied:

$$\hat{f}^m(x) = \hat{f}^{m-1}(x) + \sum_{k=1}^{n-1} \beta_k^m P_k^m(x)A_k(x) \tag{14}$$

where $x \in [a, b]$, $m \geq 1$.

Nice approximation properties of the F^m-transform can be proved. Similar to the case of the basic (zero degree) F-transform, the following can be proved: if $n \to \infty$, where n is the number of basic functions $A_1, \ldots, A_{n-1}$, then the obtained sequence of inverse F^m-transforms $\hat{f}_{(n)}^m$ of f, where $m \geq 1$, uniformly converges to f (see [21] for the details).

The following lemmas will be useful later.

Lemma 1
Let $F_0^0[f], \ldots, F_n^0[f]$ be components of the F^0-transform w.r.t an h-uniform fuzzy partition $A_0, \ldots, A_n \in \mathscr{F}([a, b])$. Let $\hat{f}^o$ be the inverse F-transform of f. Then

(a) $\int_a^b f(x)dx = h\left(\sum_{k=1}^{n-1} F_k^0[f] + \frac{1}{2}(F_0^0[f] + F_n^0[f])\right)$.

(b) $\int_a^b \hat{f}^0(x)\,dx = \int_a^b f(x)\,dx$.

PROOF: (a) was proved in [20] and (b) in [25].

□

Lemma 2 ([19])
Let $f : [a, b] \longrightarrow \mathbb{R}$ be a continuous function and $\hat{f}$ its inverse F-transform (both zero or first degree). Then

$$\max_{x\in[a,b]} |f(x) - \hat{f}(x)| \leq 2\omega(h, f) \tag{15}$$

where

$$\omega(h, f) = \max_{\substack{|x-y|<h \\ x,y\in[a,b]}} |f(x) - f(y)|$$

is the modulus of continuity of f.

Let us remark that for the first degree F-transform, this lemma follows from [21, Lemma 2]. Note also that if the function f is smooth "without abrupt changes in its course" then $\omega(h, f)$ is small.

3. Analysis of time series using F-transform

In this section, we assume that time series can be additively decomposed into trend cycle, seasonal component, and noise. Our main goal is to prove that the F-transform enables us to extract the trend-cycle. The basic idea is to show that there exists a fuzzy partition using which we either completely remove or significantly reduce subcomponents forming the seasonal component and also significantly reduce the noise.

3.1. Decomposition of time series

Let us consider a complex-valued stochastic process (see [1, 9])

$$X : [a, b] \times \Omega \longrightarrow \mathbb{C} \tag{16}$$

where $[a, b] \subset \mathbb{R}$ is an interval of reals and $\langle \Omega, \mathscr{A}, P\rangle$ is a probabilistic space. For simplicity, we will usually suppose that $a = 0$.

By a *time series* we understand a stochastic process where $[a, b]$ is replaced by a finite set of integers $Q = \{a, \ldots, b = p\} \subset \mathbb{N}$. Since all the results below derived for a stochastic process (16) can be also applied to time series, in our analysis below we will always consider (16) (unless stated otherwise).

It is clear from (16) that for each $t \in [a, b]$ the function $X(t, \omega)$ of ω ($\omega \in \Omega$), is a random variable. Our basic assumption is that $X(t, \omega)$ can be decomposed into three components, namely

$$X(t, \omega) = TC(t) + S(t) + R(t, \omega), \qquad t \in [a, b], \omega \in \Omega, \tag{17}$$

where TC is a *trend-cycle* and S is a seasonal component and R is a noise. Both TC and S are usual (i.e. non-random) functions of a real variable.

Furthermore, the seasonal component $S(t)$ is assumed to be a sum of complex-valued periodic functions

$$S(t) = \sum_{j=1}^{r} P_j \, e^{i(\lambda_j t+\varphi_j)} \tag{18}$$

for some finite r where λ_j are frequencies, φ_j phase shifts and P_j are amplitudes. Thus, (17) becomes

$$X(t,\omega) = TC(t) + \sum_{j=1}^{r} P_j\, e^{i(\lambda_j t+\varphi_j)} + R(t,\omega), \qquad t \in [a,b]. \tag{19}$$

To be terminologically consistent, we will refer to the functions $P_j\, e^{i(\lambda_j t+\varphi_j)}$ as to *subcomponents* of S.

The random noise $R(t,\omega)$ is assumed to be a real stationary stochastic process with zero mean and finite variance:

$$\mathbf{E}(R) = \mu = 0 \quad \text{and} \quad \mathbf{D}(R) = \sigma > 0. \tag{20}$$

In this paper, we consider the noise to be represented as the simplest possible type of a stationary stochastic process (see, e.g.,[27, Example 1]), namely, as the process of the type

$$R(t,\omega) = \xi(\omega)e^{i\lambda t+\varphi} \tag{21}$$

where ξ is a random variable with zero mean value and λ is a real number. It is known (see, e.g., [27]) that, under reasonable conditions, every stationary random process with zero mean can be represented as a linear combination of processes of type (21).

If we fix $\omega \in \Omega$ then we obtain one realization of the stochastic process (16) so that all the components in (17) become ordinary functions. Therefore, in our further analysis, we will be write simply $X(t) = TC(t)+S(t)+R(t)$ and assume that these are continuous functions.

If we apply F-transform to $X(t)$, the components of $\mathbf{F}[X]$ become

$$\mathbf{F}[X] = \mathbf{F}[TC] + \sum_{j=1}^{r} P_j \mathbf{F}[e^{i(\lambda_j t+\varphi_j)}] + \mathbf{F}[R] \tag{22}$$

by the linearity of F-transform. In the following two subsections we will show that there is a fuzzy partition such that the F-transform of the seasonal component $\sum_{j=1}^{r} P_j \mathbf{F}[e^{i(\lambda_j t+\varphi_j)}]$ is either zero or very close to it and the F-transform of the noise $\mathbf{F}[R]$ is also very small. This enables us to obtain a good estimation of the trend-cycle TC.

3.2. Removing seasonal component

3.2.1. Basic idea

Let us consider one subcomponent $Pe^{i(\lambda t+\varphi)}$ of S with the periodicity T and frequency λ where $\lambda = \frac{2\pi}{T}$ (because of the latter equality, we will, in case of need, speak freely either about λ or about T). Furthermore, let us construct a h-uniform fuzzy partition $A_0, \dots, A_n$ consisting of *triangular fuzzy sets* A_k of the width $2h$ over equidistant nodes $c_0, \dots, c_n$ where $c_{k+1} = c_k + h$, $k = 0, \dots, n-1$ with the distance $h = \frac{b-a}{n}$.

For simplicity we will assume that $a = 0$ and define the nodes $c_0, \ldots, c_n$ as follows:

$$\{c_0 = 0,\ c_1 = d\,T, \ldots, c_{k-1} = (k-1)dT,\ c_k = k\,d\,T,\ c_{k+1} = (k+1)dT, \\ \ldots, c_n = ndT = b\}, \qquad n \geq 2. \quad (23)$$

One can immediately see that the distance h between the nodes is related to the periodicity T by the simple equality

$$h = d\,T \quad (24)$$

where $d > 0$ is a suitable real number. Clearly, $h = \frac{2\pi d}{\lambda}$, i.e. $\lambda = \frac{2\pi d}{h}$. This means that for a fixed h, higher d corresponds to a higher frequency λ. We will argue below that higher frequencies are filtered out after applying the F-transform with respect to the fuzzy partition defined over the nodes (23).

3.2.2. Removing seasonal component using F^0-transform

In the following technical lemma we will compute components of the F-transform of $Pe^{i(\lambda t+\varphi)}$ with respect to the fuzzy partition over the nodes (23).

Lemma 3
Let $Pe^{i(\lambda t+\varphi)}$ be a function with the frequency λ and phase shift φ. Let us fix h and choose $d \in \mathbb{R}$ so that $h = dT$where $T = \frac{2\pi}{\lambda}$. Finally, let (23) be a set of $(n+1)$ h-equidistant nodes and $A_0, \ldots, A_n$ be a fuzzy partition over (23) such that each A_k is the triangular fuzzy set (2) having the width $2h$. Then the components of the F-transform of $Pe^{i(\lambda t+\varphi)}$ are the following:

$$F_k[Pe^{i(\lambda t+\varphi)}] = -\frac{Pe^{i\varphi}}{4d^2\pi^2}\, e^{i2(k-1)d\pi}(e^{i2d\pi} - 1)^2, \quad (25)$$

$$F_0[Pe^{i(\lambda t+\varphi)}] = \frac{Pe^{i\varphi}}{2d^2\pi^2}\left(1 - e^{i2d\pi} + i2d\pi\right), \quad (26)$$

$$F_n[Pe^{i(\lambda t+\varphi)}] = \frac{Pe^{i\varphi}}{2d^2\pi^2}\left(-e^{i2(n-1)d\pi} + e^{i2nd\pi}(1 - i2d\pi)\right). \quad (27)$$

PROOF: First, note that $x_k = \frac{2\pi kd}{\lambda}$. Then we proceed by straightforward computation: using (2) and (5), we obtain k-th component of the F-transform of $Pe^{i(\lambda t+\varphi)}$ as follows:

$$F_k[Pe^{i(\lambda t+\varphi)}] = \frac{P\lambda(k+1)}{2\pi d}\int_{\frac{2\pi kd}{\lambda}}^{\frac{2\pi(k+1)d}{\lambda}} e^{i(\lambda t+\varphi)}dt \\ - \frac{P\lambda(k-1)}{2\pi d}\int_{\frac{2\pi(k-1)d}{\lambda}}^{\frac{2\pi kd}{\lambda}} e^{i(\lambda t+\varphi)}dt + \\ + \frac{P\lambda^2}{4\pi^2d^2}\left(\int_{\frac{2\pi(k-1)d}{\lambda}}^{\frac{2\pi kd}{\lambda}} te^{i(\lambda t+\varphi)}dt - \int_{\frac{P2\pi kd}{\lambda}}^{\frac{2\pi k+1d}{\lambda}} te^{i(\lambda t+\varphi)}dt\right) \quad (28)$$

where $k \in \{1, \dots, n-1\}$. After integration we obtain formula (25) from (28). For $k = 1$ and $k = n$, we use formulas (4), which give (26) and (27).

□

As for the boundary components F_0, F_n, recall that they are computed using only halves of the corresponding basic functions A_0 and A_n. Consequently, the inverse F-transform approximates the original function in the intervals $[c_0, c_1]$ and $[c_{n-1}, c_n]$ with less precision.

Below, we will denote by $[d]$ the maximal integer part of $d \in \mathbb{R}$.

Corollary 2
Let the conditions of Lemma 3 be satisfied and $d = \frac{h}{T}$. Then for all $k = 1, \dots, n-1$:

(a)

$$\left|F_k[Pe^{i(\lambda t+\varphi)}]\right| = \frac{P\sin^2(d\pi)}{d^2\pi^2}. \tag{29}$$

(b) Let $d' := d - [d]$. Then

$$\left|F_k[Pe^{i(\lambda t+\varphi)}]\right| = \frac{P\sin^2(d'\pi)}{d^2\pi^2}. \tag{30}$$

PROOF: This follows from (25) by expanding to trigonometric form and realizing that $|e^{i\varphi}| = 1$ and $e^{i2k\pi} = 1$ for any $k \in \mathbb{N}$. □

Corollary 3
Let the conditions of Lemma 3 and Corollary 2 be satisfied. Then the following holds for any $k = 1, \dots, n-1$:

(a) $\left|F_k[Pe^{i(\lambda t+\varphi)}]\right|$ *does not depend on the phase shift φ.*

(b) $\left|F_k[Pe^{i(\lambda t+\varphi)}]\right| = \left|F_k[Pe^{i(\frac{2\pi d}{h}t+\varphi)}]\right| = 0$ *whenever $d \in \mathbb{N}$.*

(c) $\lim_{d\to\infty} |F_k[Pe^{i(\frac{2\pi d}{h}t+\varphi)}]| = 0$,

$$\lim_{d'\to 0}\left|F_k[Pe^{i(\frac{2\pi([d]+d')}{h}t+\varphi)}]\right| = 0 \quad \textit{and} \quad \lim_{d'\to 1}\left|F_k[Pe^{i(\frac{2\pi([d]+d')}{h}t+\varphi)}]\right| = 0.$$

PROOF: Immediately from Corollary 2. □

We conclude from Corollary 3 that if h is fixed and the frequency λ is increasing then, under the conditions of Lemma 3, the absolute values of F-transform components of $Pe^{i(\lambda t+\varphi)}$ are either equal to zero for $d \in \mathbb{N}$, or they converge to zero otherwise. A graph depicting behavior of $|F_k[Pe^{i(\frac{2\pi d}{h}t+\varphi)}]|$ with respect to d is in Figure 1.

It is, of course, not surprising that similar results also hold if we confine only to real valued seasonal subcomponent. For comparison, we present lemma characterizing the inverse F-transform of $\sin(\lambda t + \varphi)$. In correspondence with Definition 4 we will denote inverse F-transform of sin by $\widehat{\sin}$.

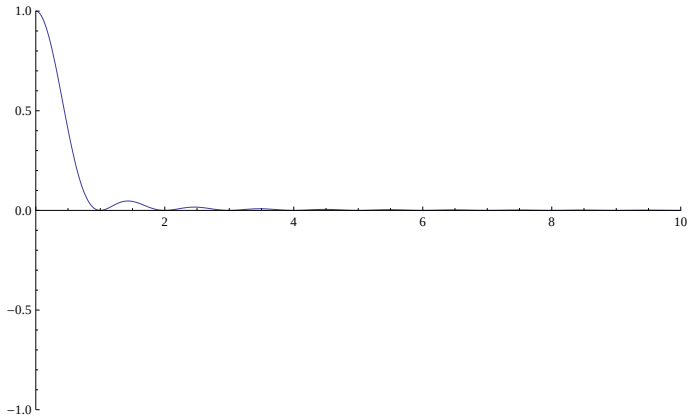

Figure 1: Graph of $|F_k[Pe^{i(\frac{2\pi d}{h}t+\varphi)}]|$ for $k \in \{1,\dots,n-1\}$ considered as a function of d ($d \in [0,10]$) where $P=1$. One can see that absolute values of each k-th component of the F-transform practically vanish for $d \geq 2$.

Lemma 4
Let $\sin(\lambda t+\varphi)$ be a function with the frequency λ and phase shift φ. Let us fix h and choose $d \in \mathbb{R}$ so that $h = dT$ where $T = \frac{2\pi}{\lambda}$. Finally, let (23) be a set of $(n+1)$ h-equidistant nodes and $A_0,\dots,A_n$ be a fuzzy partition over (23) such that each A_k is the triangular fuzzy set (2) having the width $2h$. If $d \in \mathbb{N}$ then $\widehat{\sin}(\frac{2\pi d}{h}t+\varphi) = 0$. Otherwise, let $d' = d - [d]$. Then the following inequality holds for the inverse F-transform of $\sin(\lambda t+\varphi)$:

$$|F_k[\sin(\lambda t+\varphi)]| \leq \frac{1}{d^2\pi^2}\sin\varphi, \tag{31}$$

as well as

$$|\widehat{\sin}(\lambda t+\varphi)| \leq \left|\frac{1}{d^2\pi^2}\sin\varphi\right|, \qquad t \in [c_1, c_{n-1}] \tag{32}$$

and $\lim_{d'\to 0}|\widehat{\sin}(\frac{2\pi([d]+d')}{h}t+\varphi)| = 0$ as well as $\lim_{d'\to 1}|\widehat{\sin}(\frac{2\pi([d]+d')}{h}t+\varphi)| = 0$.

PROOF: After some computation, we obtain using (2) and (5):

$$F_k[\sin(\lambda t+\varphi)] = \frac{1}{4d^2\pi^2}(2\sin(2kd'\pi)\cos\varphi + 2\cos(2kd'\pi)\sin\varphi)(1-\cos 2d'\pi) \tag{33}$$

where $d' \in [0,1]$. If $d \in \mathbb{N}$, i.e. $d'=0$, then (33) is equal to 0. Otherwise

$$\lim_{d'\to 0} F_k[\sin(\lambda t+\varphi)] = 0 \quad \text{and} \quad \lim_{d'\to 1} F_k[\sin(\lambda t+\varphi)] = 0.$$

For $d' = 0.5$ we obtain

$$F_k[\sin(\lambda t+\varphi)] = \pm\frac{1}{d^2\pi^2}\sin\varphi \tag{34}$$

where the sign depends on k, i.e. (34) is positive for k even and negative for k odd. Hence, (31) holds true.

Let $t \in [c_{k-1}, c_k]$, $k \in \{1, \dots, n-1\}$. Then

$$|\widehat{\sin}(\lambda t + \varphi)| = |A_{k-1}(t)F_{k-1}[\sin(\lambda t + \varphi)] + A_k(t)F_k[\sin(\lambda t + \varphi)]| \leq$$
$$\leq \underbrace{(A_{k-1}(t) + A_k(t))}_{=1} \left| \frac{1}{d^2\pi^2} \sin\varphi \right|. \quad (35)$$

Since the right-hand side does not depend on k, we obtain (32).

□

3.2.3. Removing seasonal component using F^1-transform

In [16], we suggested that the F^1-transform may improve estimation of the trend-cycle. Therefore, with respect to the above results we must ask whether the F^1-transform removes seasonal periodic components as well. The answer is positive as follows from the sequence of lemmas below.

Recall that we consider nodes of the h-uniform fuzzy partition in the form $c_k = \frac{2\pi kd}{\lambda}$, $k = 0, \dots, n$. Furthermore, unlike the basic (i.e. F^0-) F-transform, components of the F^1-transform are linear functions

$$F_k^1[Pe^{i(\lambda t+\varphi)}](t) = F_k^0[Pe^{i(\lambda t+\varphi)}] + \beta_k^1 \left(t - \frac{2\pi kd}{\lambda} \right) \quad (36)$$

where the coefficients β_k^1 are computed using formula (11). The variable $t \in (-\infty, \infty)$. However, since in (13) we multiply each k-th component by $A_k(t)$ which equals zero for all $t \notin (c_{k-1}, c_{k+1})$, it makes sense to consider the k-th component only for $t \in [c_{k-1}, c_{k+1}]$.

Lemma 5
Let $Pe^{i(\lambda t+\varphi)}$ be a function with the frequency λ and phase shift φ. Let us fix h and choose $d \in \mathbb{R}$ so that $h = dT$ where $T = \frac{2\pi}{\lambda}$. Finally, let (23) be a set of $(n+1)$ h-equidistant nodes and $A_0, \dots, A_n$ be a fuzzy partition over (23) such that each A_k is the triangular fuzzy set (2) having the width $2h$. Then for each $k = 1, \dots, n-1$ and $t \in [c_{k-1}, c_{k+1}]$ we obtain:

(a)

$$F_k^1[Pe^{i(\lambda t+\varphi)}](t) =$$
$$= \frac{Pe^{i\varphi}}{d^4\pi^4} \sin d\pi \cdot (i3d\pi(2dk\pi - \lambda t)\cos d\pi + (d\pi(d\pi - i6k) + i3\lambda t)\sin d\pi). \quad (37)$$

(b)

$$\left| F_k^1[Pe^{i(\lambda t+\varphi)}](t) \right| =$$
$$= \frac{P\sin^2 d\pi}{d^4\pi^4} \cdot \sqrt{d^4\pi^4 \sin^2 d\pi + 9(\lambda t - 2dk\pi)^2(\sin d\pi - d\pi\cos d\pi)^2}. \quad (38)$$

(c) Expression (38) can be slightly simplified by putting $d = [d] + d'$:

$$\left|F_k^1[Pe^{i(\lambda t+\varphi)}](t)\right| = \\ = \frac{P\sin^2 d'\pi}{d^4\pi^4}\cdot\sqrt{d^4\pi^4\sin^2 d'\pi + 9(\lambda t - 2dk\pi)^2(\sin d'\pi - d\pi\cos d'\pi)^2}. \tag{39}$$

PROOF: The proof is similar to the proof of Lemma 3, by straightforward computation using (11). □

Similar to the case of F^0-transform, we obtain the following:

Corollary 4
Let the conditions of Lemma 5 be satisfied. Then the following holds for any $k = 1, \dots, n-1$ and $t \in [c_{k-1}, c_{k+1}]$:

(a) If $d \in \mathbb{N}$ then $F_k^1[Pe^{i(\frac{2\pi d}{h}t+\varphi)}](t) = 0$.

(b) $\left|F_k^1[Pe^{i(\lambda t+\varphi)}](t)\right|$ does not depend on the phase shift φ.

(c) $\lim_{d\to\infty}\left|F_k^1[Pe^{i(\frac{2\pi d}{h}t+\varphi)}](t)\right| = 0$ and

$$\lim_{d'\to 0}\left|F_k^1[Pe^{i(\frac{2\pi([d]+d')}{h}t+\varphi)}](t)\right| = 0 \quad \text{and} \quad \lim_{d'\to 1}\left|F_k^1[Pe^{i(\frac{2\pi([d]+d')}{h}t+\varphi)}](t)\right| = 0.$$

PROOF: Immediately from Lemma 5 by straightforward computation. □

Let us also investigate the behavior of $F_k^1[Pe^{i(\lambda t+\varphi)}]$ on an interval $[c_{k-1}, c_{k+1}] = \left[\frac{2\pi(k-1)d}{\lambda}, \frac{2\pi(k+1)d}{\lambda}\right]$. It is convenient to transform t in (36) into an auxiliary variable $t' \in [-1, 1]$ by setting $t = c_k + h\,t' = \frac{2\pi d}{\lambda}t'$. Then (36) can be written, for the given k, as the function

$$F_k^1[Pe^{i(\lambda t+\varphi)}](t') = F_k^0[Pe^{i(\lambda t+\varphi)}] + \beta_k^1\frac{2\pi d}{\lambda}t', \qquad t' \in [-1, 1]. \tag{40}$$

Lemma 6
Let the conditions of Lemma 5 be satisfied, Then for each $k = 1, \dots, n-1$ and $t' \in [-1, 1]$ we have:

(a)

$$F_k^1[Pe^{i(\lambda t+\varphi)}](t') = \frac{Pe^{i\varphi}}{d^3\pi^3}\,\sin d\pi\,((d\pi + i6t')\sin d\pi - i6d\pi t'\cos d\pi). \tag{41}$$

(b)

$$\left|F_k^1[Pe^{i(\lambda t+\varphi)}](t')\right| = \left|\frac{Pd\sin(d'\pi)}{d^4\pi^3}\right|\cdot \\ \cdot\sqrt{d^2\pi^2\sin^2 d'\pi + 6(t'\sin d'\pi - d\pi t'\cos d'\pi)^2}. \tag{42}$$

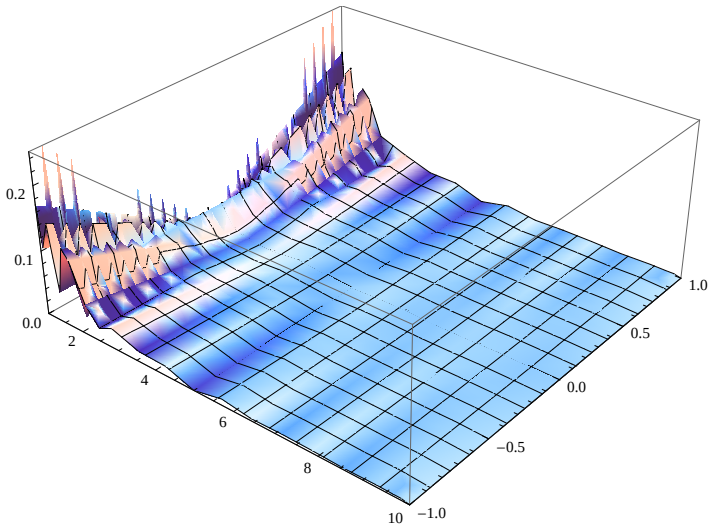

Figure 2: Graph of $|F_k^1[Pe^{i(\lambda t+\varphi)}]|$ where $k \in \{1,\dots,n-1\}$ and $P=1$ as a function of d ($d \in [0,10]$) and t' ($t' \in [-1,1]$). One can see that absolute values of each k-th component of the F^1-transform also practically vanish for $d \geq 2$.

PROOF: This follows from (40) by straightforward computation similar to the proof of Lemma 5. □

A graph depicting behavior of the absolute value of F_k^1 with respect to d is in Fig. 2. A graph depicting behavior of the absolute value of F_k^1 for $t' \in [-1,1]$ with respect to the remainder $d' = d - [d]$ is in Figure 3. One can see that $\left|F_k^1[Pe^{i(\lambda t+\varphi)}](t')\right|$ is a very small number for all $t' \in [-1,1]$.

3.3. Reducing noise

In this subsection, we will discuss how the F-transform can eliminate the random noise $R(t,\omega)$. We will prove that the use of F-transform drastically decreases the noise of the type (21). As stated above, under reasonable conditions, every stationary random process with zero mean can be represented as a linear combination of processes of type (21) (see, e.g., [27]). Because of the linearity of F-transform, we can therefore conclude that, in the general case, the use of F-transform drastically decreases each subcomponent (21) of the random noise.

Theorem 2
Let $R(t,\omega)$ be a random noise satisfying (20), $A_0,\dots,A_n$ be a uniform fuzzy partition over $[a,b]$ and $\mathbf{F}^0[R]$ be a direct F^0-transform of R. Then

(a) $\mathbf{E}(F_k^0[R]) = \mu$ *for all* $k = 1,\dots,n-1$,

(b) $\mathbf{E}(\hat{R}^0(t)) = \mu$ *for all* $t \in [c_1, c_{n-1}]$.

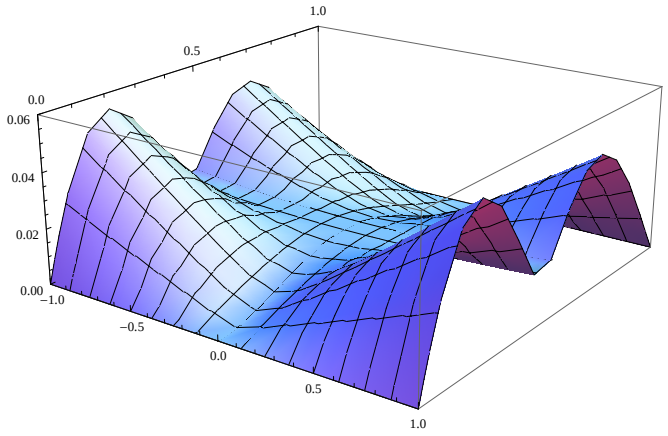

Figure 3: Graph of the detail of $|F_k^1[Pe^{i(\lambda t+\varphi)}]|$ where $P = 1$ and $[d] = 2$ as a function of t' ($t' \in [-1, 1]$) and the remainder values d' ($d' \in [0, 1]$).

PROOF: (c) Using (5) and the assumption (20) we have

$$\mathbf{E}(F_k^0[R]) = \frac{1}{h}\mathbf{E}\left(\int_{c_{k-1}}^{c_{k+1}} A_k(t)R(t)dt\right) = \frac{1}{h}\int_{c_{k-1}}^{c_{k+1}} A_k(t)\mathbf{E}(R(t))dt =$$
$$= \frac{1}{h}\mu\int_{c_{k-1}}^{c_{k+1}} A_k(t)dt = \mu.$$

(d) Using (b), we obtain $\mathbf{E}(\hat{R}^0(t)) = \sum_{k=0}^{n} A_k(t)\mathbf{E}(R(t)) = \mu\sum_{k=0}^{n} A_k(t) = \mu$ for all $t \in [c_1, c_{n-1}]$. □

Let us now consider one realization $R(t)$ for a fixed ω. First, we assume that the noise $R(t)$ has the form (21). Then for each $t \in [a, b]$, there exist one realization of $\xi(t)$. Put $\bar{\xi} = \sup\{\xi(t) \mid t \in [a, b]\}$ and $\underline{\xi} = \inf\{\xi(t) \mid t \in [a, b]\}$. Finally, we put

$$\tilde{\xi} = \begin{cases} \bar{\xi} & \text{if } \bar{\xi} \geq 0, \\ \underline{\xi} & \text{if } \bar{\xi} < 0. \end{cases} \tag{43}$$

Theorem 3
Let $R(t)$ be a noise represented by formula (21), $A_0, \ldots, A_n$ be an h-uniform fuzzy partition over $[a, b]$ fulfilling conditions of Lemma 3, $\mathbf{F}^0[R]$ be a direct and $\hat{R}^0$ an inverse F^0-transform of R. Then for each $k = 1, \ldots, n-1$

$$|F_k^0[R]| \leq \frac{|\tilde{\xi}|\sin^2(d\pi)}{d^2\pi^2}, \tag{44}$$

as well as

$$|\hat{R}^0| \leq \frac{|\tilde{\xi}|\sin^2(d\pi)}{d^2\pi^2}, \qquad t \in [c_1, c_{n-1}] \tag{45}$$

where d is related to h via (24).

PROOF: By the linearity of the F-transform we have either

$$F_k^0[R(t)] \leq \bar{\xi} \cdot F_k[e^{i\lambda t+\varphi}]$$

if $\bar{\xi} \geq 0$ or

$$F_k^0[R(t)] \geq \underline{\xi} \cdot F_k[e^{i\lambda t+\varphi}]$$

if $\bar{\xi} < 0$. Hence,

$$|F_k^0[R(t)]| \leq |\tilde{\xi}| \cdot |F_k^0[e^{i\lambda t+\varphi}]| \leq \frac{|\tilde{\xi}| \sin^2(d\pi)}{d^2\pi^2} \tag{46}$$

by (29).

Inequality (45) is obtained as follows:

$$|\hat{R}^0(t)| = \left|A_{k-1}(t)\,\tilde{\xi}\,F_{k-1}^0[e^{i\lambda t+\varphi}] + A_k(t)\,\tilde{\xi}\,F_k^0[e^{i\lambda t+\varphi}]\right| \leq$$

$$\leq \underbrace{(A_{k-1}(t) + A_k(t))}_{=1} \frac{|\tilde{\xi}| \sin^2(d\pi)}{d^2\pi^2}.$$

□

Theorem 4
Let $R(t)$ be a noise represented by formula (21), $A_0, \ldots, A_n$ be an h-uniform fuzzy partition over $[a, b]$ fulfilling conditions of Lemma 5. Let d be related to h via (24), $\mathbf{F}^1[R]$ be a direct and $\hat{R}^1$ an inverse F^1-transform of R. Then for each $k = 1, \ldots, n-1$ and $t \in [c_1, c_{n-1}]$

$$|F_k^1[R](t)| \leq \frac{|\tilde{\xi}| \sin^2 d\pi}{d^4\pi^4} \cdot \tag{47}$$

$$\cdot \sqrt{d^4\pi^4 \sin^2 d\pi + 9(\lambda t - 2dk\pi)^2(\sin d\pi - d\pi \cos d\pi)^2}, \tag{48}$$

as well as

$$|\hat{R}^1| \leq |\tilde{\xi}| \cdot \eta(t), \qquad t \in [c_1, c_{n-1}] \tag{49}$$

where

$$\eta(t) = \frac{\sin^2(d\pi)}{d^4\pi^4} \cdot \max\left\{\sqrt{d^4\pi^4 \sin^2 d\pi + 9(\lambda t - 2dk\pi)^2(\sin d\pi - d\pi \cos d\pi)^2}\right|$$

$$k = 1, \ldots, n-1\Big\}. \tag{50}$$

PROOF: This follows from Lemma 5 analogously as in Theorem 3. □

3.4. Estimation of the trend-cycle using F-transform

In this subsection we will show that on the basis of the results in the previous two sections, we can apply the F-transform (both zero and first-degree) to estimation of the trend-cycle. The following is assumed:

(i) The stochastic process X can be decomposed as in (19) where the seasonal component S consists of periodic functions having periodicities T_j, $j \in \{1, \dots, r\}$ (see (18)). We take a fixed ω and consider one realization of $X(t)$.

(ii) Put $\bar{T} = \max\{T_j \mid j = 1, \dots, r\}$, choose a number $\bar{d} \in \mathbb{N}$ and set the distance h in (23) between the nodes to

$$h = \bar{d}\bar{T} \tag{51}$$

so that $n \geq 2$. Then, form the corresponding triangular fuzzy partition $A_0, \dots, A_n$.

(iii) The trend-cycle TC is a function with no clear periodicity or its periodicity is much longer than $\bar{h}$. Moreover, the modulus of continuity $\omega(h, TC)$ is small.

Note that (iii) requires that TC is smooth with small changes in its course.

The following theorem provides estimation of the inverse F-transform $\hat{S}$ of the seasonal component S.

Theorem 5
Let $S(t)$ be the seasonal component (18) whose members have periodicities T_j, $j = 1, \dots, r$. Furthermore, let an h-uniform fuzzy partition $A_0, \dots, A_n$ be formed over the equidistant set of nodes (23) with the distance $h = \bar{d}\bar{T}$ where $\bar{T}$ is the longest periodicity among all T_j, $j \in \{1, \dots, r\}$.

(a) Let $d_j = \frac{h}{T_j} \in \mathbb{N}$ for all $j = 1, \dots, r$. Then $\hat{S}^0(t) = 0$ as well as $\hat{S}^1(t) = 0$ for all $t \in [c_1, c_{n-1}]$.

(b) Let $I \subset \{1, \dots, r\}$ be a set of subscripts for which $d'_j = d_j - [d_j] \in (0, 1)$, $j \in I$. Then the following holds for all $t \in [c_1, c_{n-1}]$:

(ba)

$$|\hat{S}^0(t)| \leq \sum_{j \in I} \left| \frac{P_j \sin^2(d'_j \pi)}{d_j^2 \pi^2} \right|, \tag{52}$$

(bb)

$$|\hat{S}^1(t)| \leq \sum_{j \in I} P_j \cdot \eta_j(t) \tag{53}$$

where

$$\eta_j(t) = \max\left\{ \frac{\sin^2 d'_j\pi}{d_j^4\pi^4}\cdot \right.$$
$$\left.\cdot\sqrt{d_j^4\pi^4\sin^2 d'_j\pi + 9(\lambda t - 2d_jk\pi)^2(\sin d'_j\pi - d_j\pi\cos d'_j\pi)^2}\,\middle|\, k=1,\dots,n-1\right\}.$$

PROOF: (a) Follows immediately from Corollaries 3(b) and 4(b).

(ba) Using Corollary 3(b) we, similarly to (35), obtain for all $t\in[c_{k-1},c_k]$ and $k=2,\dots,n-1$

$$|\hat{S}^0(t)| = \left|\sum_{k=0}^{n} A_k(t)F_k^0[S]\right| = \left|\sum_{k=0}^{n} A_k(t)\sum_{j\in I} F_k^0[P_j e^{i(\lambda_j t+\varphi_j)}]\right| =$$
$$\left|\sum_{j\in I}\sum_{k=0}^{n} A_k(t)\,F_k[P_j e^{i(\lambda_j t+\varphi_j)}]\right| \le \sum_{j\in I}\sum_{k=0}^{n} A_k(t)\,|F_k^0[P_j e^{i(\lambda_j t+\varphi_j)}]| \le$$
$$\le \sum_{j\in I} |A_{k-1}(t)F_{k-1}^0[P_j e^{i(\lambda_j t+\varphi_j)}] + A_k(t)F_k^0[P_j e^{i(\lambda_j t+\varphi_j)}]| \le$$
$$\le \sum_{j\in I} \underbrace{(A_{k-1}(t)+A_k(t))}_{=1}\left|\frac{P_j\sin^2(d'_j\pi)}{d_j^2\pi^2}\right|$$

from which (52) follows.

(bb) is proved in a similar way using Lemma 5(c). □

It follows from Corrolaries 3 and 4 that the right hand sides of (52) and (53) are very small numbers (many summands are even equal to zero). Let us now denote

$$D^0 = \sum_{j\in I}\left|\frac{P_j\sin^2(d'_j\pi)}{d_j^2\pi^2}\right| + \frac{|\tilde{\xi}|\sin^2(d\pi)}{d^2\pi^2}, \tag{54}$$
$$D^1 = \sum_{j\in I}\sum_{j\in I}\eta_j(t) + |\tilde{\xi}|\cdot\eta(t) \tag{55}$$

where $d_j = \frac{h}{T_j}$ and $I\subset\{1,\dots,r\}$ is the set of all subscripts, for which $d'_j = d_j - [d_j]\in(0,1)$, $\tilde{\xi}$ is determined in (43) and $\eta(t)$ is given by (50). The following theorem provides estimation of the error when extracting the trend cycle TC from the time series $X(t)$ using the F-transform.

Theorem 6
Let $X(t)$ be realization of the stochastic process in (17) considered over the interval $[0,b]$. If we construct a fuzzy partition over the set of equidistant nodes (23) with the distance (51) then the corresponding inverse F-transform of $X(t)$ gives the following estimator $\hat{X}^m$ of the trend-cycle with the error:

$$|\hat{X}^m(t) - TC(t)| \le 2\omega(h, TC) + D^m, \qquad t\in[c_1,c_{n-1}], \tag{56}$$

where D^m, $m \in \{0,1\}$, is the error (54) or (55), respectively depending on the degree of the applied F-transform.

PROOF: The theorem is a consequence of Lemma 2 and Theorems 5, 3, and 4. □

Recall that, by the assumption, the modulus of continuity $\omega(h, TC)$ is also a small number. Taking into account Theorem 5, we conclude from Theorem 6 that the *F-transform enables us to extract the trend-cycle TC from the time series $X(t)$ with high accuracy.*

It follows from the method described in Subsections 3.2.2 and 3.2.3 that, as a byproduct, we can also extract subcomponents forming the seasonal component. This will be demonstrated in the following section.

4. Experimental verification

In this section we will demonstrate how the above described F-transform trend estimation method works on data[2]. We will also compare it with three classical methods for analysis of time series.

4.1. Three selected classical methods

To compare F-transform with other classical methods that are frequently used in the analysis of time series, we chose the following three non-parametric ones: STL-method, Butterworth low-pass filter and Singular Spectrum Analysis. Let briefly outline the main ideas of these methods.

STL-method (Season-Trend-Loess regression) is a filtering procedure for decomposing a time series into three components (17). The procedure consists of a sequence of applications of the loess regression method (locally weighted regression — see [5]). First, the trend is estimated using the loess regression. Then a sequence of subseries forming the seasonal component is separated and detrended. All these steps are realized in the, so called, inner loops. Finally, the outer loop is run resulting in the estimation of noise. The Loess regression is applied several times during the procedure. Recall that this is a classical regression limited to a narrow window represented by a special weight function. Note that this function has similar properties as the basic function of the fuzzy transform (cf. Definition 1) and so, it be taken as a fuzzy set shifted along the data. The STL-method is quite complicated and has a high computational complexity. Detailed description of the method including some examples can be found in [4].

The *Butterworth filter* (see [3, 10, 26]) is a name for a wider class of filters that can be used as a low-pass, high-pass and band-pass ones. The main idea of the low-pass filter is to remove components of the time series that have

[2]The reader can verify our results as well as analysis and forecasting of time series using our experimental software *LFL Forecaster* whose β-version is available on our WEB page http://irafm.osu.cz under Research/Software.

frequencies above a given cutoff frequency λ_c. Recall that response function of the filter (as a function of frequency) is determined as a fraction of the amplitude of the output series at frequency λ divided by the amplitude of the input series at the same frequency. The low-pass Butterworth filter has the response function

$$G(\lambda)^2 = \frac{1}{1 + (\frac{\lambda}{\lambda_c})^{2n}} \tag{57}$$

where the parameter n influences sharpness of the cutoff. Thus, for frequencies lower than λ_c is (57) close to 1 and for higher is close to 0.

The main idea of the *Singular Spectrum Analysis* (SSA) technique (see [8, 11]) is also to decompose the original time series into the components (17). The SSA technique consists of two complementary stages: At the first stage, the time series is decomposed into so-called elementary matrices using a singular value decomposition of the trajectory matrix constructed upon the time series. At the second stage, the original time series is reconstructed as a sum of diagonal averaged matrices that are derived by summing the elementary matrices splitted into several groups. Neither a parametric model nor stationarity are assumed for the time series.

Using the F-transform and the above mentioned classical methods we ran tests on two kinds of data: (1) two artificially formed time series whose structure is exactly known, and (2) three real time series taken from Internet (Time Series Data Library): (a) *monthly Canadian unemployment figures in the years 1956–1975* (thousands), (b) *monthly Number of slaughtered pigs in Victoria in the years 1980–1995*, (c) *monthly Accidental deaths in the USA in the years 1973-1978*.[3].

4.2. Artificial time series

Comparison of the methods on artificially formed time series is the most convincing way how to justify strength of the methods (of course, besides precise mathematical proofs, if available) because we know exactly structure of the time series and so, we can see how the given method estimated the real known component. Therefore, we formed two artificial time series on the set of integers $t \in \{0, \dots, 100\}$ as follows:

1. *Time series AS1* is formed as follows:

$$\begin{aligned} X(t) = 20 \sin 0.063t + 5 \sin(0.63t + 1.5) + 5 \sin(1.26t + 0.35) \\ + 15 \sin(2.7t + 1.12) + 7 \cos(0.41t + 0.79) + R(t) \end{aligned} \tag{58}$$

   where the trend-cycle is modeled by the first sin function $TC(t) = 20 \sin 0.063t$ that has periodicity 100. The other four sine members form the seasonal component $S(t)$. Their periodicities are $T_1 = 10$, $T_2 = 5$, $T_3 = 2.3$, $T_4 = 15.4$, respectively. The $R(t)$ is a random noise with average $\bar{\mu} = -0.24$.

[3] This time series is considered also in [11].

2. *Time series AS2* differs from AS1 only in the trend-cycle:

$$X(t) = TC(t) + 5\sin(0.63t + 1.5) + 5\sin(1.26t + 0.35) + 15\sin(2.7t + 1.12) + 7\cos(0.41t + 0.79) + R(t) \quad (59)$$

where the trend-cycle $TC(t)$ is given by artificial data *without clear periodicity*. Its modulus of continuity is $\omega(30, TC) = 3.22$.

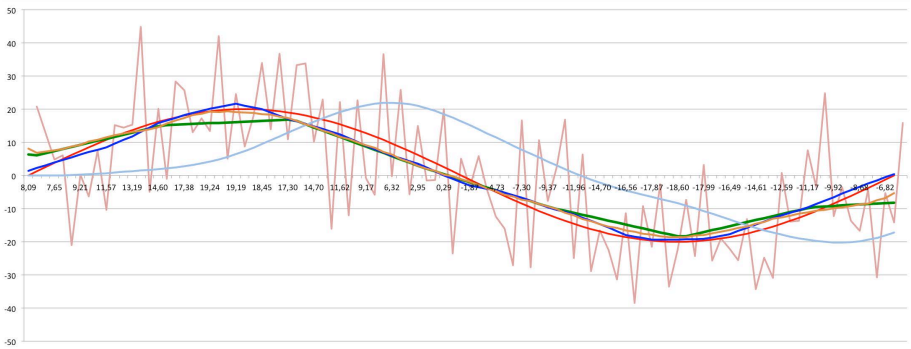

Figure 4: Demonstration of the trend-cycle estimation of the artificial time series AS1. The original trend cycle, given by sine function with periodicity 100, is depicted by red line. The estimated trend-cycle using various methods is depicted as follows: F^0-transform — green line; STL-method — blue line; Butterworth filter — light blue line; and SSA-method — yellow line.

In accordance with the theoretical results above, we estimated the trend-cycle of these time series using F-transform as follows: we set $\bar{T} = T_4$ and $d = 1$, i.e. the distance (51) between nodes is $h = 15$ (the time axis is discrete and so, fractions are neglected). Consequently, width of the basic functions is $2h = 30$. Since all $d_1, \ldots, d_4$ are close to natural numbers, the error D^0 in (54) is very close to 0. Let us remark that periodogram applied to both artificial time series reliably detected all the real periodicities.

Artificial time series AS1. Results of trend-cycle estimation are depicted in Figures 4 and 5. The known real trend-cycle is depicted in both figures by red line. Figure 4 contains estimation of the trend-cycle using F^0-transform, STL-method, SSA-method, and Butterworth low-pass filter. Figure 5 contains comparison of the trend estimation using both F^0- and F^1-transforms. As expected, the F^1-transform is smoother and more precise.

Numerical comparison of all tested methods with respect to the real trend-cycle of the series AS1 using RMSE (Root Mean Square Error) measure is the following:

Method	F^0-transform	F^1-transform	STL	SSA	Butterworth
RMSE	3.13	1.82	1.90	2.52	12.03

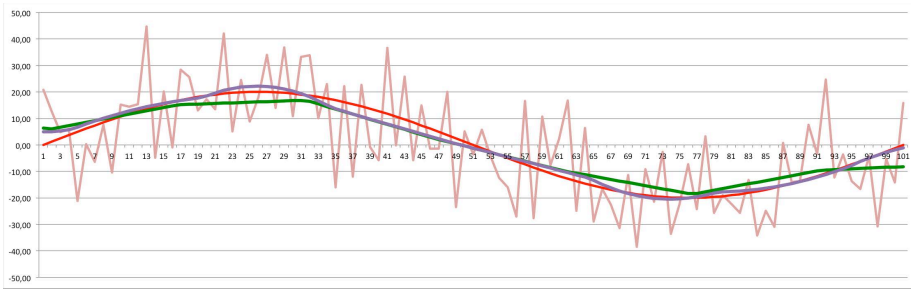

Figure 5: Comparison of the known trend-cycle (red line) of the artificial time series AS1 with its estimation using both F^0- (green line) and F^1-transform (violet line).

It can be seen from the figures and this table that the results of the F-transform, STL and SSA methods are comparable. The F^0-transform is slightly worse than the other two classical methods because its inverse F-transform is partially linear; the F^1 transform approximates the real trend-cycle with the best precision.

As can be seen, the F^0-transform is able to remove the whole seasonal component including noise almost completely. The maximal difference between the inverse F-transform and the real trend-cycle is

$$\max_{t\in\{0,100\}} |\, TC(t) - \hat{X}^0(t)| = 3.32.$$

We may thus conclude that the trend-cycle was estimated with the error corresponding to (56) (cf. also (15)). Note that the Butterworth filter does not give convincing results though its cutoff frequency crresponds to (58).

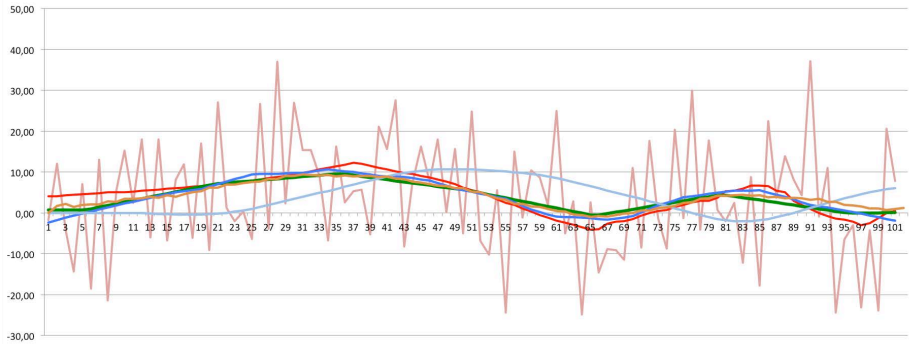

Figure 6: Demonstration of the trend-cycle estimation of the artificial time series AS2 whose trend-cycle is a function without clear periodicity. The original known trend cycle is depicted by red line. The estimated trend-cycle using various methods is depicted as follows: F^0-transform — green line; STL-method — blue line; Butterworth filter — light blue line; SSA-method — yellow line.

Artificial time series AS2. Results of comparison of the trend-cycle estimation of the artificial time series AS2 using all four methods are depicted in Figure 6. Numerical comparison with respect to the real trend-cycle using RMSE measure is the following:

Method	F^0-transform	F^1-transform	STL	SSA	Butterworth
RMSE	2.08	1.79	1.95	1.88	6.07

One can see that the results are similar to those of AS1.

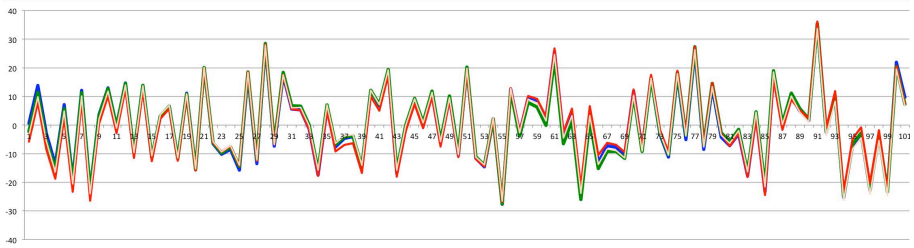

Figure 7: The seasonal component (including noise) of the artificial time series AS2 and its estimation using F^0-transform, STL- and SSA-methods. The original component $S(t) + R(t)$ is red and its estimations are: F^0 transform is green, STL-method is blue and SSA-method is light brown.

We also compared estimation of the combined seasonal and noise component $S(t) + R(t)$ using all three methods. In case of the F^0-transform, we obtained it by "detrending" the original time-series. The other two methods provide the components $S(t)$ and $R(t)$ separately. The results are in Figure 7. One can see that estimation of the seasonal component using all three methods is quite good — the difference between real $S(t)+R(t)$ and its estimations is almost invisible. The RMSE measure of STL is 1.95, that of F^0-transform is 2.09 and that of SSA is 1.88. So, the difference in RMSE among the methods is insignificant.

To demonstrate the power of the F-transform, we also estimated the second sine subcomponent with the periodicity 15 that is contained in the component $S(t) + R(t)$ (cf. (59)). This was obtained from the estimation of $S(t) + R(t)$ by "detrending" the time series (cf. Figure 7) and setting the distance between nodes to $h = \bar{T} = 10$.

4.3. Real time series

To see how the F-transform works on real time series, we chose three time series introduced in Subsection 4.1. All of them seem to have a clear trend cycle and also a clear seasonal component. However, the precise trend-cycle of these time series is not known and, therefore, we cannot measure quality of the results.

We compared F^0-transform with all three classical methods considered above. We used periodogram to detect the periodicities and according to its results, we

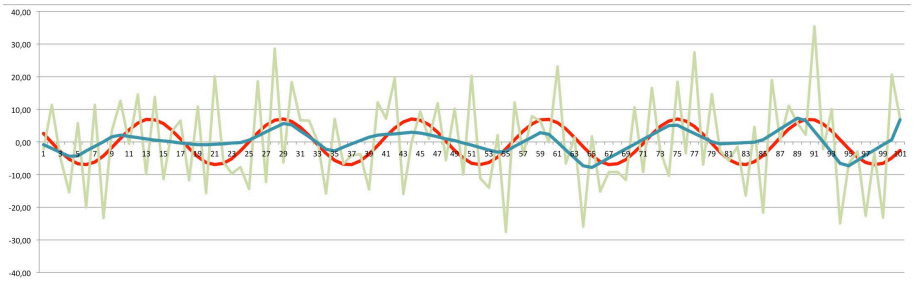

Figure 8: Estimation of the sine component with periodicity $T = 15$ from the seasonal component $S(t)$ (including noise) using the F^0-transform. The $S(t) + R(t)$ component is light green, the original sine component is red and its estimation using F^0-transform is blue.

set distance between the nodes of the F-transform as follows: Canadian unemployment figures $h = 34$ (i.e., width of the basic functions is 68), Pigs $h = 31$ (width of the basic functions is 62) and Accidental deaths $h = 12$ (width of the basic functions is 24). To be able to compare F-transform with the other methods, we set their parameters in accordance with the width of the basic functions. The results are in Figure 9.

One can see that analogously to the case of artificial time series, the F^0-transform, STL and SSA methods give similar estimation while the Butterworth low pass filter is clearly worse.

5. Conclusion

This paper is devoted to theoretical analysis of the F-transform applied to time series under the assumption that the latter can be additively decomposed into three components: trend-cycle, seasonal component and random noise. We proved several theorems which demonstrate that the seasonal component can be eliminated by application of the F-transform. Moreover, if the random noise is stationary with zero (or very small) mean value μ then it can be significantly reduced. Therefore, our results lead to the conclusion that the F-transform is a convenient tool using which the trend-cycle, as informally characterized by OECD, can be extracted. Unlike classical parametric statistical approaches where the trend-cycle is assumed in advance to be some specific simple function (quite often linear), the F-transform does not use any predefined shape and still provides exact formula for computation of the trend-cycle.

We compared the F-transform with three classical non-parametric methods, namely STL method, SSA method, and Butterworth low pass filter. The comparison was realized on two artificial time series whose structure is exactly known and also on three real time series. In all cases, the F-transform turned out to be fully comparable with STL and SSA-methods.

As already emphasized, the big advantage of the F-transform is its transparentness, relative simplicity and small computational complexity. The transpar-

Figure 9: Estimation of the trend-cycle of 3 real time series: Canadian unemployment figures (up), Monthly slaughtered pigs (middle) and Monthly accidental deaths (down). Estimations of these methods are depicted as follows: F^0-transform — green line; STL-method — orange line; Butterworth filter — light blue line; SSA-method — yellow line.

entness and simplicity is given by the fact that the F-transform is determined by a simple uniform fuzzy partition that can be easily specified and when modified, we immediately see the effect of our modification. Moreover, unlike both STL and SSA methods, the F-transform provides also analytic formula for the estimated trend-cycle (formulas (6) or (13)).

Further investigation will focus on analysis of the correspondence between parameters of the F-transform and various statistical characteristics of the given time series. On the basis of the demonstrated properties of the F-transform, we will also try to find a method for forecasting of seasonal component. Finally, we will study influence of the missing values of the time series on its resulting inverse F-transform.

Acknowledgment

The authors thank to Dr. Michal Burda who prepared the classical methods (STL, SSA and Butterworth) in R system and realized all the computations presented in this paper. We also thank to anonymous reviewers whose comments significantly helped to improve this paper.

References

[1] J. Anděl, Statistical Analysis of Time Series, SNTL, Praha, 1976 (in Czech).

[2] A. Bovas, J. Ledolter, Statistical Methods for Forecasting, Wiley, New York, 2003.

[3] S. Butterworth, On the theory of filter amplifiers, Experimental Wireless and the Wireless Engineer 7 (1930) 536–541.

[4] R. Cleveland, W. Cleveland, J. E. McRae, I. Terpenning, Stl: A seasonal-trend decomposition procedure based on Loess, Journal of Official Statistics 6 (2006) 3–73.

[5] S. Cleveland, S. Devlin, Locally-weighted regression: An approach to regression analysis by local fitting, Journal of the American Statistical Association 83 (1988) 596–610.

[6] J. Fan, Q. Yao, Nonlinear time series. Nonparametric and parametric methods., New York, NY: Springer, 2003.

[7] J. Gao, Nonlinear times series: semiparametric and nonparametric methods., Boca Raton, FL: Chapman & Hall/CRC, 2007.

[8] N. Golyandina, A. Zhigljavsky, Singular spectrum analysis for time series, SpringerBriefs in Statistics, Springer, Berlin, 2013.

[9] J. Hamilton, Time Series Analysis, Princeton, Princeton University Press, 1994.

[10] A. Harvey, T. Trimbur, General model-based filters for extracting cycles and trends in economic time series, Review of Economics and Statistics 85 (2003) 244–255.

[11] H. Hassani, Singular spectrum analysis: Methodology and comparison, Journal of Data Science 5 (2007) 239–257.

[12] M. Holčapek, T. Tichý, A smoothing filter based on fuzzy transform, Fuzzy Sets and Systems 180 (2011) 69–97.

[13] B. Kedem, K. Fokianos, Regression Models for Time Series Analysis, J. Wiley, New York, 2002.

[14] V. Martin, S. Hurn, D. Harris, Econometric modelling with time series. Specification, estimation and testing., Cambridge: Cambridge University Press, 2013.

[15] V. Novák, I. Perfilieva, V. Krejnovich, F-transform in the analysis of periodic signals, in: M. Inuiguchi, Y. Kusunoki, M. Seki (Eds.), Proc. 15^{th} Czech-Japan Seminar on Data Analysis and Decision Making under Uncertainty, Osaka University, Osaka, Japan, 2012, pp. 150–158.

[16] V. Novák, I. Perfilieva, V. Pavliska, The use of higher-order F-transform in time series analysis, in: World Congress IFSA 2011 and AFSS 2011, Surabaya, Indonesia, 2011, pp. 2211–2216.

[17] V. Novák, M. Štěpnička, A. Dvořák, I. Perfilieva, V. Pavliska, L. Vavříčková, Analysis of seasonal time series using fuzzy approach, Int. Journal of General Systems 39 (2010) 305–328.

[18] V. Novák, M. Štěpnička, I. Perfilieva, V. Pavliska, Analysis of periodical time series using soft computing methods, in: D. Ruan, J. Montero, J. Lu, L. Martínez, P. D'hondt, E. Kerre (Eds.), Computational Intelligence in Decision and Control, World Scientific, New Jersey, 2008, pp. 55–60.

[19] I. Perfilieva, Fuzzy transforms: theory and applications, Fuzzy Sets and Systems 157 (2006) 993–1023.

[20] I. Perfilieva, Fuzzy transforms: A challenge to conventional transforms, in: P. Hawkes (Ed.), Advances in Images and Electron Physics, 147, Elsevier Academic Press, San Diego, 2007, pp. 137–196.

[21] I. Perfilieva, M. Daňková, B. Bede, Towards a higher degree F-transform, Fuzzy Sets and Systems 180 (2011) 3–19.

[22] I. Perfilieva, P. Hurtík, F. DiMartino, S. Sessa, Image reduction method based on the F-transform, Transactions on Image Processing (2014) (to appear).

[23] I. Perfilieva, R. Valášek, Fuzzy transforms in removing noise, in: B. Reusch (Ed.), Computational Intelligence, Theory and Applications, Springer, Heidelberg, 2005, pp. 225–234.

[24] S. W. Smith, The Scientist & Engineer's Guide to Digital Signal Processing, California Technical Pub, 1997.

[25] L. Stefanini, F-transform with parametric generalized fuzzy partitions, Fuzzy Sets and Systems 180 (2011) 98–120.

[26] W. A. Woodward, H. L. Gray, A. C. Elliott, Applied time series analysis., Boca Raton, FL: CRC Press, 2012.

[27] A. Yaglom, An introduction to the theory of stationary random functions. Revised English ed. Translated and edited by Richard A. Silverman., Englewood Cliffs, NJ: Prentice-Hall, Inc. XIII, 1962.